PNAS RESEARCH ARTICLE | NEUROSCIENCE

An extracellular scaffolding complex confers unusual rectification upon an ionotropic acetylcholine receptor in *C. elegans*

Maëlle Jospin[a,1], Benjamin Bonneau[b,2], Viviane Lainé[b], and Jean-Louis Bessereau[a]

Edited by Jean-Pierre Changeux, Institut Pasteur, Paris, France; received November 22, 2021; accepted May 8, 2022

Biophysical properties of ligand-gated receptors can be profoundly modified by auxiliary subunits or by the lipid microenvironment of the membrane. Hence, it is sometimes challenging to relate the properties of receptors reconstituted in heterologous expression systems to those of their native counterparts. Here we show that the properties of *Caenorhabditis elegans* levamisole-sensitive acetylcholine receptors (L-AChRs), the ionotropic acetylcholine receptors targeted by the cholinergic anthelmintic levamisole at neuromuscular junctions, can be profoundly modified by their clustering machinery. We uncovered that L-AChRs exhibit a strong outward rectification in vivo, which was not previously described in heterologous systems. This unusual feature for an ionotropic AChR is abolished by disrupting the interaction of the receptors with the extracellular complex required for their synaptic clustering. When recorded at −60 mV, levamisole-induced currents are similar in the wild type and in L-AChR-clustering–defective mutants, while they are halved in these mutants at more depolarized physiological membrane potentials. Consequently, levamisole causes a strong muscle depolarization in the wild type, which leads to complete inactivation of the voltage-gated calcium channels and to an irreversible flaccid paralysis. In mutants defective for L-AChR clustering, the levamisole-induced depolarization is weaker, allowing voltage-gated calcium channels to remain partially active, which eventually leads to adaptation and survival of the worms. This explains why historical screens for *C. elegans* mutants resistant to levamisole identified the components of the L-AChR clustering machinery, in addition to proteins required for receptor biosynthesis or efficacy. This work further emphasizes the importance of pursuing ligand-gated channel characterization in their native environment.

acetylcholine receptor | *C. elegans* | clustering | rectification

Significance

At chemical synapses, the biophysical properties of ionotropic neurotransmitter receptors play a major role in neuronal communication. These properties are mainly determined by intrinsic features of the channel pore-forming subunits and by interactions with auxiliary subunits. In this study we show that a cholinergic receptor in the model organism *C. elegans* exhibits a strong voltage dependence, which can only be observed when receptors are associated with their clustering machinery. This very unusual behavior for such receptors has a strong impact on the actions of agonists at the organism level, including a dramatic change in the effect of the widely used pest control levamisole. Hence, our work emphasizes the need to study how endogenous factors influence ion channel function.

The electrical properties of ligand-gated receptors are specified by the structure of the pore-forming subunits but they are also greatly influenced by non-pore-forming auxiliary subunits. Stargazin was the first protein associated with glutamatergic AMPA receptors that fulfills criteria for an auxiliary subunit (i.e., directly and stably interacting with the pore-forming subunits, modifying receptor properties, being required for receptor function in vivo, and not contributing to the pore of the channel) (1, 2). Since then, numerous other auxiliary proteins have been identified for ligand-gated receptors (3–9), including acetylcholine receptors (10, 11). The diversity of auxiliary subunits accounts for the broad variety of electrical properties recorded in vivo for ligand-gated receptors, which is poorly recapitulated in heterologous systems expressing only a minimal set of subunits. These discrepancies highlight the need to study ion channel properties in their native environment, but also emphasize the challenge of defining the relevant molecular composition of receptors in vivo.

Cutting-edge proteomic techniques are extremely efficient to detect receptor-associated proteins (12, 13), yet unbiased genetic strategies can identify key components regulating the activity of receptors in vivo independently of the strength of the interaction. A good example is the analysis of levamisole-sensitive acetylcholine receptors (L-AChRs) in the nematode *Caenorhabditis elegans*. Levamisole is a widely used anthelminthic that activates heteromeric ligand-gated nicotinic AChRs, present at worm neuromuscular junctions (NMJs) (14–19). L-AChRs are composed of three alpha subunits, UNC-63, UNC-38, LEV-8, and two nonalpha subunits, UNC-29 and LEV-1 (20–23). At high concentrations, it causes an irreversible paralysis and kills the worms. Unbiased genetic screens identified a large set of mutants that can survive high levamisole concentration, leading to the identification of new proteins required for L-AChR function (see for review (24)). These proteins are involved in biosynthesis, trafficking (22, 25–28) or gating of the receptors, such as MOLO-1, an auxiliary subunit tightly associated with L-AChRs that enhances channel gating and is required for

Author contributions: M.J. and J.L.B. designed research; M.J., B.B., and V.L. performed research; B.B. and V.L. contributed new reagents/analytic tools; M.J. and V.L. analyzed data; and M.J. and J.L.B. wrote the paper.

The authors declare no competing interest.

This article is a PNAS Direct Submission.

[1]To whom correspondence may be addressed. Email: maelle.jospin@univ-lyon1.fr.

[2]Present address: Univ Paris-Saclay, CNRS UMR3347, INSERM U-102, Institut Curie, F-91405 Orsay, France.

This article contains supporting information online at http://www.pnas.org/lookup/suppl/doi:10.1073/pnas.2113545119/-/DCSupplemental.

Published July 12, 2022.

normal receptor function (10). In addition to identifying mutants that have fewer or less functional L-AChRs, screens for levamisole resistance have also led to the identification of mutants impaired for receptor clustering (29–31).

In *C. elegans*, clustering of L-AChRs at NMJs requires an unusual extracellular scaffold composed of at least three proteins expressed by the postsynaptic muscle cells (Fig. 1*A*): LEV-10, LEV-9, and OIG-4 (29–31). These three proteins form a complex with L-AChR, and the disruption of any of these proteins causes a disruption of the clusters and the diffusion of nonclustered L-AChRs along the muscle membrane. L-AChRs-containing clusters are localized at cholinergic NMJs by the extracellular matrix protein MADD-4/Ce-Punctin, an anterograde synaptic organizer secreted by motor neurons that controls the composition of the synaptomatrix and the differentiation of postsynaptic domain (32, 33).

The levamisole resistance of *lev-9*, *lev-10*, and *oig-4* null mutants, hereafter referred to as clustering-defective mutants, raises a paradox: electrophysiological experiments have shown that levamisole-induced currents are similar in wild type and in mutants (29–31), so these results predict that both strains

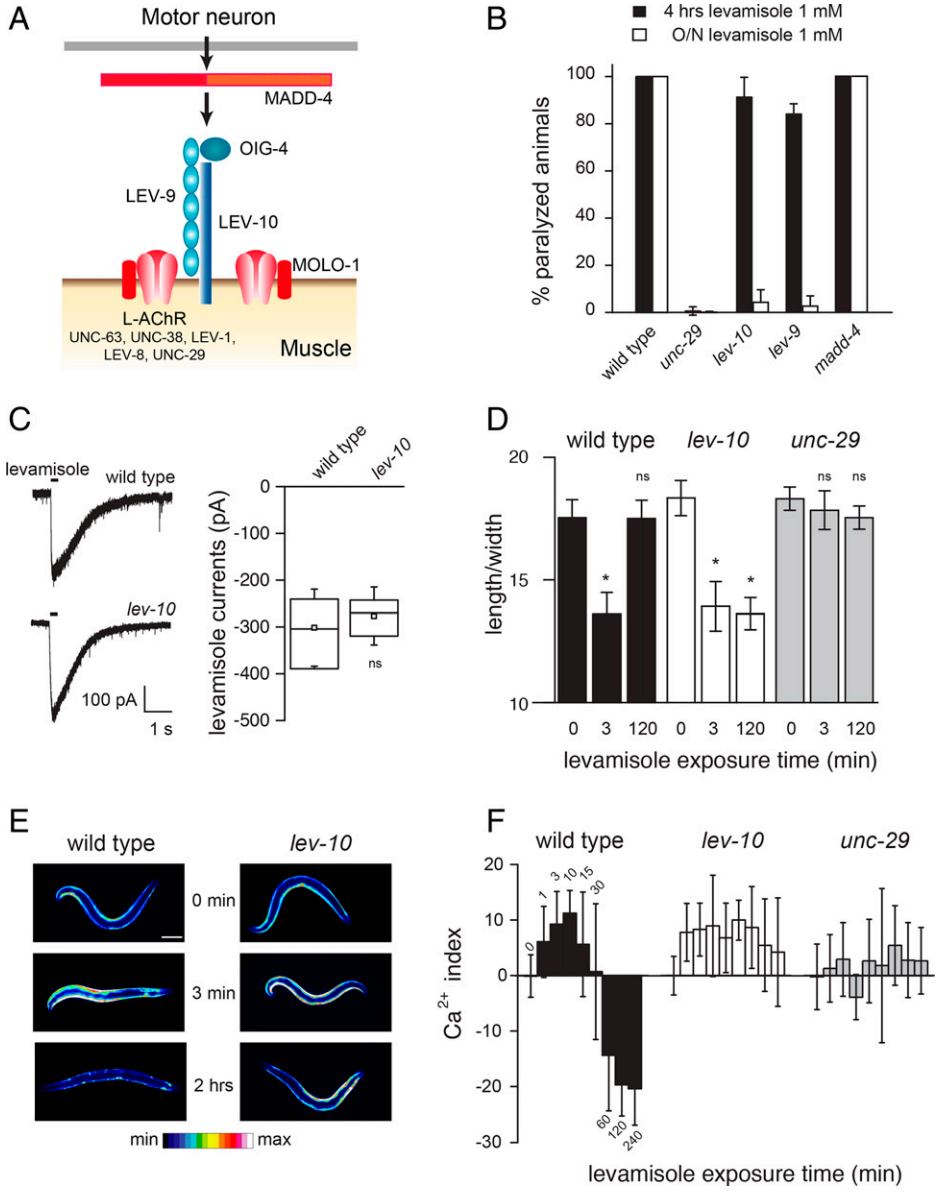

Fig. 1. Levamisole induces different behavioral responses in wild type and *lev-10* but elicits same current on muscle cells. (*A*) Schematic of L-AChR clustering machinery. MADD-4/Ce-Punctin is secreted by motor neurons and localizes the heteromeric AChRs composed of UNC-38, UNC-63, LEV-1, LEV-8, and UNC-29. LEV-10, OIG-4, and LEV-9 are part of the clustering machinery. MOLO-1 is an L-AChR auxiliary subunit. (*B*) Percentage of paralyzed animals at 4 h and after overnight exposure to levamisole 1 mM. Mean values ± SD were plotted (wild type, $n = 6$; *unc-29*, $n = 8$; *lev-10*, $n = 8$; *lev-9*, $n = 6$; and *madd-4*, $n = 3$, where n is the number of independent experiments; to total number of animals tested per genotype: 60 to 160). (*C*) Representative traces and mean amplitude of currents evoked by 0.1 mM pressure-ejected levamisole on muscle cells hold at −60 mV. In this figure and all the figures, bar represents median, square represents mean, boxes represent quartiles, and whiskers represent SD. Student *t* test $P = 0.36$ (wild type, $n = 19$; *lev-10*, $n = 13$). (*D*) Morphologic data for wild type, *lev-10*, and *unc-29* before and during exposure to 1 mM levamisole ($n = 8$ for the 3 genotypes except at 120 min for wild type and *unc-29*, $n = 7$). The ratio was compared using 1-way ANOVA at 0, 3, and 120 min for wild type ($P < 0.0001$), *lev-10* ($P < 0.0001$), and *unc-29* ($P = 0.07$) followed by Holm-Sidak posttests: ns, nonsignificant, $^*P < 0.05$. (*E*) Representative pictures of wild type and *lev-10* mutants expressing GCaMP3 in body muscles before (0) or after 3 and 120 min-exposure to 1 mM levamisole (16-color lookup table). Scale bar is 0.1 mm. (*F*) Calcium imaging data for wild type, *lev-10*, and *unc-29* mutants during levamisole exposure. Young adults expressing GCaMP3 in body muscle were imaged on regular NGM (Nematode Growth Medium) plates at t = 0 min and were then put on 1 mM levamisole plates. Different cohorts of animals have been imaged at 0, 1, 3, 10, 15, 30, 60, 120, and 240 min of levamisole exposure, $n > 15$ for each genotype at each time point except at 10 min for *lev-10* and *unc-29*, $n = 9$ and $n = 10$, respectively (see also *SI Appendix*, Table S1). The calcium index was calculated as indicated in *Material and Methods*. Mean currents ± SD were plotted.

should be equally sensitive to levamisole, which is not the case (16). Here, we reinvestigated this 40-y-old paradox and we show that the extracellular clustering complex associated with L-AChRs confers strong outward rectification to these receptors, thus potentiating the effect of levamisole at more depolarized potentials. This, in turn, modifies the response of muscle cells and, eventually, the capability of the worms to survive high concentrations of the anthelmintic drug levamisole.

Results

Levamisole Causes Different Behavioral Responses in Wild Type and L-AChR-Clustering–Defective Mutants Despite the Induction of Similar Currents in Muscle Cells. The functionality of L-AChRs can be assessed in vivo by analyzing the behavioral response of animals exposed to high concentration of levamisole. As previously described (16), we observed that wild type and L-AChR-clustering–defective mutants, such as *lev-9* and *lev-10* null mutants, initially contracted and were paralyzed when placed on 1 mM levamisole plates. However, whereas wild-type animals remained paralyzed, *lev-9* and *lev-10* mutants recovered locomotion after ∼8 h, a phenomenon called adaptation to levamisole (Fig. 1*B* and *SI Appendix*, Fig. S1*A*). Despite their different behaviors, pressure-ejected levamisole elicited similar currents in muscle cells clamped at −60 mV in wild type and *lev-10* mutants (Fig. 1*C*; see also (29)). By contrast, animals that did not express L-AChRs in muscle, such as null mutants for the L-AChR subunit UNC-29 (20), never became paralyzed in the presence of 1 mM levamisole (Fig. 1*B* and *SI Appendix*, Fig. S1*A*).

Mutating *lev-9* or *lev-10* has two different consequences on L-AChRs. First, it disrupts the clustering machinery and frees receptors from interactions with components of this extracellular complex. Second, receptors relocalize outside of synaptic zones. To test if the adaptation of levamisole is dependent on L-AChR clustering or on synaptic localization, we analyzed *madd-4* null mutant where L-AChRs still associate with the clustering machinery but are no longer retained at synapses (32). *madd-4* mutants behaved like wild-type worms (Fig. 1*B*), suggesting that the lack of association with the clustering machinery and not the synaptic localization is required for levamisole adaptation.

L-AChR-Clustering–Defective Mutants Maintain Muscle Contraction upon Prolonged Exposure to Levamisole. Observations of wild type and mutants during levamisole exposure suggested that a difference in the response to levamisole might occur earlier than the recovery of locomotion. As described in detail by Lewis and collaborators (16), wild-type animals rapidly contract on 1 mM levamisole plates, leading to a spastic paralysis. This phase is followed by a complete relaxation of the body-wall muscle cells and a flaccid paralysis. At that stage, animals can still recover locomotion in a few hours if removed from levamisole (*SI Appendix*, Fig. S1*B*). In contrast, L-AChR-clustering–defective mutants remain contracted, as shown by measurement of the length/width ratio over time (Fig. 1*D*). As a control, we observed no variation of this ratio with levamisole-resistant *unc-29* mutants that lack L-AChRs (Fig. 1*D*).

We hypothesized that the variations of muscle contraction mirrored the evolution of calcium concentrations. We therefore directly monitored intracellular calcium levels during levamisole exposure using GCaMP3 expressed in muscle (Fig. 1*E*). To analyze the evolution of calcium in the entire muscle population of each genotype, we imaged worms at low magnification and calculated a calcium index. It corresponds to the variation of pixel number above a threshold defining the upper quartile of pixel intensities measured in the absence of levamisole. As expected in strains expressing no L-AChR, such as *unc-29* or *unc-63* mutants, the calcium index did not vary during levamisole exposure (Fig. 1*F* and *SI Appendix*, Table S1). In sensitive strains, such as wild type and *madd-4*, and adapting strains, such as *lev-9*, *lev-10*, and *molo-1*, the calcium index increased as soon as the worms were exposed to levamisole and reached a maximal value after ∼10 min. Then it started to decrease in sensitive strains and reached negative values after 1 h, in agreement with the observed flaccid paralysis. By contrast, the calcium index remained relatively stable for up to 4 h in the adapting strains (Fig. 1*F* and *SI Appendix*, Table S1).

Taken together, behavioral and calcium imaging data reveal that the muscle response to levamisole differs between wild type and the clustering-defective strains within the first hour of exposure to levamisole: muscle cells from mutants maintain contraction and high levels of calcium over time while the wild-type muscles relax after 30 min of exposure.

L-AChRs Are Still Active in Wild Type after Prolonged Exposure to Levamisole. We wondered why calcium decreased after 30 min of levamisole exposure in wild type muscle but not in adapting mutants. We first hypothesized that L-AChRs might desensitize or be inhibited in the wild type but not in the clustering-defective mutants. To test this hypothesis, we recorded muscle membrane potentials in wild-type and *lev-10* animals before or after a 1-h exposure to 1 mM levamisole. In the absence of levamisole, the membrane potentials of wild type and *lev-10* were similar (−20 ± 3 mV and −23 ± 4 mV respectively; mean ± SD). After levamisole exposure, the membrane potentials were depolarized in both cases (Fig. 2*A*). This depolarization was not due to an unspecific leakage current because the L-AChR blocker d-tubocurarine (dTBC) was able to repolarize the cells (Fig. 2*B*). We concluded from these results that the decrease of calcium observed in wild-type muscles after 1 h of levamisole treatment was not caused by selective inhibition of clustered L-AChRs versus declustered receptors.

Disrupting the L-AChR Clustering Machinery Modifies the Electrophysiological Response to Levamisole in a Voltage-Dependent Manner. An unexpected observation came out from the previous experiment: levamisole-induced depolarization was in fact stronger in wild type than in *lev-10* (−5 ± 4 mV and −13 ± 4 mV, respectively, mean ± SD). This result was surprising since levamisole-induced currents were of similar amplitude between wild type and *lev-10* (Fig. 1*C* and (29)). However, in each case, levamisole-induced currents were recorded at −60 mV. This is far from the resting membrane potential of striated muscle in *C. elegans*, which is established around −20 mV as shown in Fig. 2*A* and in previous studies (34–36). We therefore wondered whether levamisole-induced currents could differ between wild type and *lev-10* at more physiological potentials. To test this hypothesis, we first applied 0.01 mM levamisole on the open-cut preparation using a perfusion system to mimic a sustained stimulation. We isolated L-AChR-dependent currents by recording levamisole responses in the presence or absence of the blocker dTBC at different potentials. While dTBC-sensitive currents were linear in *lev-10*, they exhibit a strong outward rectification in the wild type. Currents were not different at −60 mV between both genotypes, but

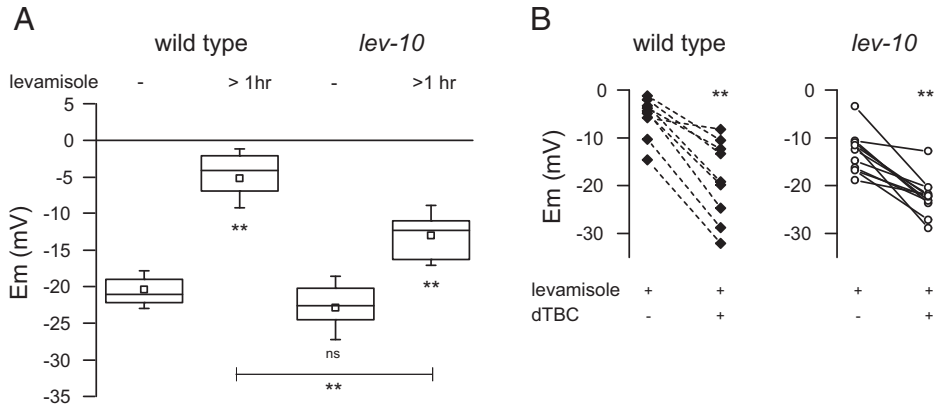

Fig. 2. L-AChR are still activated in wild type and *lev-10* after 1 h of 1 mM levamisole exposure. (*A*) Membrane resting potentials of muscle cells in wild type (n = 14), *lev-10* (n = 14), wild type exposed to 1 mM levamisole during 1 h (n = 12), and *lev-10* exposed to 1 mM levamisole during 1 h (n = 14). For animals placed on levamisole plates, levamisole was also added in the external solution at the concentration of 0.01 mM; ANOVA, $P < 0.0001$; Holm-Sidak posttests, $P < 0.001$ for all except for wild type/*lev-10* without levamisole. (*B*) Effect of dTBC on membrane resting potentials of muscle cells in wild type (n = 9) and *lev-10* (n = 9) exposed to 1 mM levamisole. Animals were placed on 1 mM levamisole plates for 1 h; levamisole was also added in the external medium at the concentration of 0.01 mM. dTBC at 0.1 mM was perfused while membrane potential was recorded. dTBC induced a significant repolarization of muscle cells in wild type and *lev-10* (paired sample test, $P = 0.0001$ and $P = 0.0004$, respectively).

they were 60% smaller in *lev-10* than in wild type at −20 mV (Fig. 3*A*). The larger current in the wild type could thus explain the more intense depolarization observed in these animals compared to *lev-10*.

Second, we explored whether similar differences could be observed with shorter levamisole applications. We went back to pressure-ejection protocol and recorded currents at −60 mV and −20 mV. In the wild type, the currents recorded at −20 mV represented 93% of that at −60 mV, while in *lev-10* mutants it was 48%. In the two other known mutants that disrupt the L-AChR-clustering complex, *lev-9* and *oig-4*, we also observed a lack of rectification ($I_{-20\ mV}/I_{-60\ mV}$ equal 46% and 43%, respectively). By contrast, in *madd-4* mutants, where L-AChRs remain associated with the clustering complex despite extrasynaptic localization, a strong outward rectification remained ($I_{-20\ mV}/I_{-60\ mV}$ equals 104%). We also analyzed *molo-1* mutants that adapt to levamisole, because they express L-AChRs with reduced open probability due to the lack of an auxiliary subunit (10). L-AChRs are still clustered at the synapse and associate with the clustering complex. A strong outward rectification was observed as in the wild type ($I_{-20\ mV}/I_{-60\ mV}$ equals 99%).

At *C. elegans* NMJs, muscle cells send dendritic-like projections, called muscle arms, toward the motor neuron axons where excitatory and inhibitory synapses are established. Thus, clustered L-AChRs are at the extremity of the muscle arms while the patch pipette is sealed on the muscle belly. In the clustering-defective mutants, L-AChRs are spread on the muscle membrane, likely including the belly (37). So, we wondered if this peculiar geometry could contribute to the nonlinear component of the current–voltage relationship. To test this hypothesis, we recorded the currents from the other receptors present at the tip of muscle arms, the type A GABA receptors encoded by *unc-49* and the homomeric alpha7-like AChR, encoded by *acr-16* and called N-AChR for nicotine-sensitive receptors (18). In both cases, we did not observe any rectification of the currents (*SI Appendix*, Fig. S2), suggesting that L-AChR rectification is not linked to muscle cell geometry.

L-AChRs Exhibit an Outward Rectification Depending on the Association with Their Clustering Machinery. The mechanism of L-AChR activation by levamisole is not known at the structural level, and levamisole also behaves as an open channel blocker at high concentrations (above 30 μM) (38). We therefore tested whether the rectification of the currents was specific to levamisole or was a general feature of the receptors. We pressure-ejected acetylcholine onto muscles of wild type and *lev-10* mutants and recorded the resulting current at −60 mV and −20 mV. Again, we observed a strong rectification of the current in the wild type but not in *lev-10* mutants (Fig. 3*C*). Contrary to levamisole, acetylcholine is easy to wash from the extracellular medium and we could build the current–potential relationship of the acetylcholine-evoked current from −60 to −10 mV (Fig. 3*D*). The outward rectification was readily visible. We could not establish the current–potential relationship above 0 mV because of the activation of large voltage-dependent potassium currents. We tried to inhibit them by adding tetraethylammonium in the extracellular solution; unfortunately, it also blocked currents flowing through L-AChRs.

To rule out that the rectification was due to a secondary-activated current, we recorded the pressure-ejected currents at −60 and −10 mV in different solutions while removing or decreasing external calcium, magnesium, sodium, or chloride concentrations (Fig. 3*E*). In all external media, the mean rectification index of L-AChR current from wild type muscle was above 0.8 while a theoretical index of 0.33 is expected if the conductance is constant, as in *lev-10* (rectification index of 0.34). Since L-AChR can be expressed in *Xenopus* oocytes, we attempted to reconstitute the L-AChR-clustering complex by coexpressing LEV-9, LEV-10, and OIG-4. We observed no difference between acetylcholine-induced currents from oocytes expressing only L-AChR subunits and those expressing L-AChR together with L-AChR-clustering proteins (*SI Appendix*, Fig. S3). However, these results are unconclusive because we have no means to test if the clustering complex assembles, especially because LEV-9 and OIG-4 are secreted and might not reach sufficient concentration for stable scaffolding interactions.

Finally, we tested if currents through L-AChR also rectified in more physiological conditions by recording the currents evoked by motor neuron stimulation in wild type, at −60 and −20 mV. Again, a strong rectification was observed (Fig. 3*F*).

Altogether, these data demonstrate that L-AChRs exhibit an outward rectification in their native physiological environment, and that this rectification is lost upon disruption with its associated clustering complex.

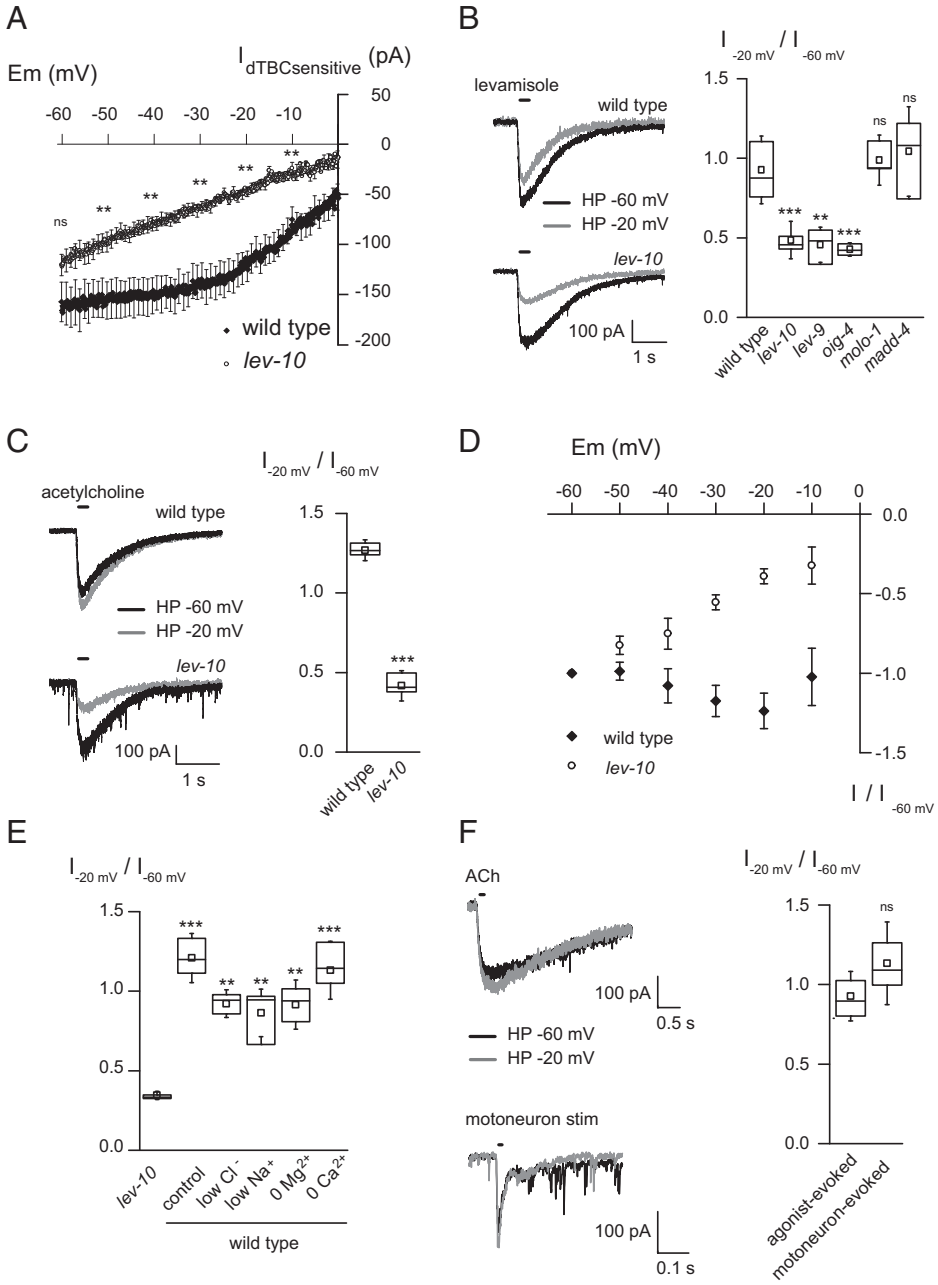

Fig. 3. Currents evoked by levamisole or acetylcholine exhibit an outward rectification, absent in *lev-10*. (*A*) dTBC-sensitive currents of muscle cells in wild type (n = 14) and *lev-10* (n = 13) in response to the perfusion of 0.01 mM levamisole. Worms grown on regular plates were dissected and currents were recorded in standard saline solutions, in the presence of 0.01 mM levamisole and in the presence of 0.01 mM levamisole and 0.1 mM dTBC. dTBC-sensitive currents were obtained by subtracting the currents in the presence of levamisole and dTBC to those in the presence of levamisole. Mean currents ± SEM were plotted. For visualization clarity, SEM were only plotted every 10 points. Currents were not different at −60 mV (Mann-Whitney test, P = 0.17) but were smaller in *lev-10* muscle cells for the other potentials (Mann-Whitney tests, P = 0.17, 0.007, 0.0003, 0.0005, 0.0005, 0.0008, and 0.03 at −50, −40, −30, −20, −10 and 0 mV, respectively). (*B*) Representative traces of currents evoked by 0.1 mM pressure-ejected levamisole on muscle cells held at −60 mV or −20 mV in wild type and *lev-10*, and fraction of current elicited by pressure-ejected levamisole at −20 mV compared to that at −60 mV in wild type (n = 21), *lev-10* (n = 12), *lev-9* (n = 6), *oig-4* (n = 8), *molo-1* (n = 5), and *madd-4* (n = 10); Kruskal Wallis, P < 0.0001; Dunn's posttests, P < 0.0001 for wild type/*lev-10*, wild type/*oig-4*, P < 0.001 for wild type/*lev-9*, P > 0.05 for wild type/*molo-1*, and wild type/*madd-4*. (*C*) Representative traces of currents evoked by 0.1 mM pressure-ejected acetylcholine on muscle cells held at −60 mV or −20 mV in wild type and *lev-10* in the presence of 0.01 mM DHβE in the external medium and fraction of current elicited by pressure-ejected acetylcholine at −20 mV compared to that at −60 mV in wild type (n = 10), *lev-10* (n = 11); Student t test, P < 0.0001. (*D*) Mean current–voltage relationship ± SD established at the peak of the currents elicited by 0.1 mM pressure-ejected acetylcholine from wild-type animals (n = 7) or *lev-10* mutants (n = 6) in the presence of 0.01 mM DHβE in the external medium. For each cell, currents at the different potentials were normalized to that at −60 mV. (*E*) Fraction of current elicited by 0.1 mM pressure-ejected acetylcholine at −20 mV compared to that at −60 mV in *lev-10* mutants (n = 9) and wild-type animals in the presence of different extracellular solutions: control (n = 15), low Cl^- (n = 6), low Na^+ (n = 11), without Mg^{2+} (n = 8), or without Ca^{2+} (n = 6) (see *Materials and Methods* for detailed compositions). DhβE 0.01 mM was present in all external media; Kruskal-Wallis, P < 0.0001, followed by Dunn's posttests: P < 0.0001 for *lev-10*/control and *lev-10*/0 Ca^{2+}, P < 0.01 for *lev-10*/0 Mg^{2+}, *lev-10*/low Na^+, *lev-10*/low Cl^-. (*F*) Representative traces of currents evoked by 0.1 mM pressure-ejected acetylcholine or cholinergic motor neuron light-induced depolarization from muscle cells held at −60 mV or −20 mV in wild type in the presence of 0.01 mM DHβE in the external medium and fraction of currents elicited by 0.1 mM pressure-ejected acetylcholine (n = 7) or following cholinergic motor neuron light-induced depolarization (n = 12) at −20 mV compared to that at −60 mV in wild-type worms in the presence of 0.01 mM DHβE in the external medium. Student t test, P = 0.07.

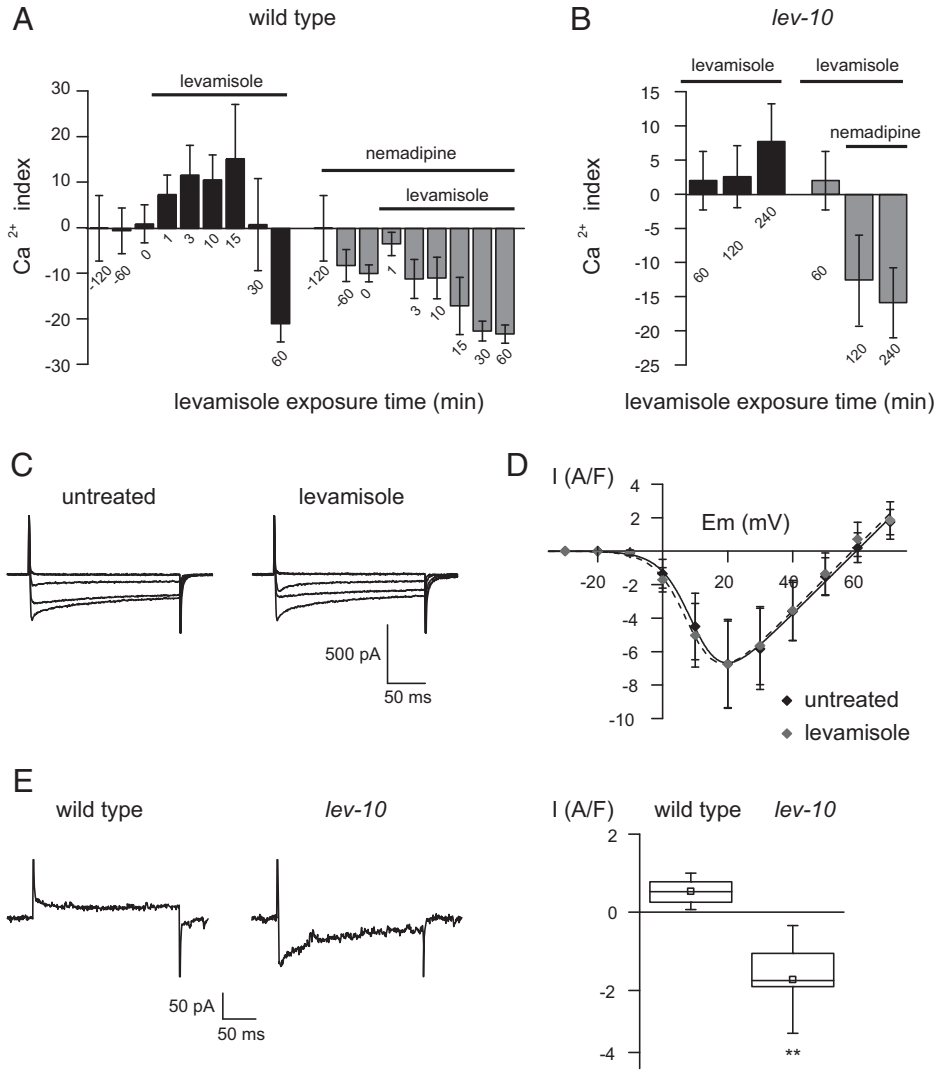

Fig. 4. VGCC are present on the membrane of muscle cells in wild type but are inactivated. (*A*) Calcium imaging data for wild type during levamisole exposure without or with nemadipine pretreatment. Animals were put on NGM plates with 0.1% DMSO or with 0.01 mM nemadipine for 2 h. They were then transferred on plates containing either 1 mM levamisole or 1 mM levamisole and 0.01 mM nemadipine. Different cohorts have been imaged at the different times (n = 9, 8, 8, 9, 8, and 10 at 0, 1, 3, 10, 15, 30, and 60 min, respectively, for animals without nemadipine; n = 9, 8, 8, 10, 9, and 9 at 0, 1, 3, 10, 15, 30, and 60 min, respectively, for animals treated with nemadipine). The calcium index was calculated as indicated in *Material and Methods*. Animals treated with nemadipine exhibited a calcium index significantly lower than that of wild type except at 60 min (Mann-Whitney test, P = 0.0008, 0.0004, 0.0009, 0.0009, 0.0003, 0.0006, and 0.06 at 0, 1, 3, 10, 15, 30, and 60 min, respectively). Mean values ± SD were plotted. (*B*) Calcium imaging data for *lev-10* during nemadipine exposure after levamisole treatment. Animals were put on 1 mM levamisole plates during 1 h and then transferred either on 1 mM levamisole plates and 0.1% DMSO or on plates containing 1 mM levamisole and 0.01 mM nemadipine. Calcium index was measured from different cohorts after 60 min of levamisole (n = 18), then after posttreatment with DMSO (n = 16 and n = 14 at t_{120} and t_{240}, respectively) or with DMSO and nemadipine (n = 20 and n = 18 at t_{120} and t_{240}, respectively). Animals posttreated with nemadipine exhibited a calcium index significantly lower than that of nontreated animals (Mann-Whitney test, $P < 0.0001$ at t_{120} and t_{240}). Mean values ± SD were plotted. (*C*) Representative traces of inward currents recorded from body muscles of wild type exposed or not (untreated) to 1 mM levamisole during 1 h in response to depolarizing pulses from −60 mV to −20, 0, +20, and +40 mV. (*D*) Mean current–voltage relationship ± SD established at the peak of the currents from untreated animals (n = 13) or from animals that spent 2 to 3 h on 1 mM levamisole plates (n = 12). For animals treated with levamisole, levamisole was kept in the external medium at the concentration of 0.01 mM. No difference was observed between treated and untreated animals (Mann-Whitney test, $P > 0.05$ for all potentials). (*E*) Representative traces and mean amplitude of inward currents recorded on muscle cells of wild-type and *lev-10* animals (n = 10 for each) exposed to 1 h of 1 mM levamisole. After obtaining whole-cell configuration, resting membrane potential was measured and the cell was then voltage-clamped at this potential and depolarized to −20 mV. Mann-Whitney test, P = 0.0004.

Voltage-Gated Calcium Channels (VGCC) Are Inactivated after Prolonged Exposure to Levamisole in the Wild Type but not in the L-AChR-Clustering–Defective Mutants. The smaller amplitude of the levamisole-induced current observed in *lev-10* mutants at physiological membrane potentials could impact signaling downstream of the receptors. Since calcium concentration decreases in wild type but not in mutants, we hypothesized that L-type VGCC might directly be involved because they are responsible for calcium transients in *C. elegans* striated muscle cells (35, 36). First, we checked whether these channels participate in the intracellular calcium concentration changes during levamisole exposure. We treated wild-type animals with nemadipine, a selective blocker of L-type VGCC (39), before exposure to levamisole. As expected, nemadipine led to a decrease of calcium index (Fig. 4*A*). Subsequent application of levamisole had only a transient impact on the calcium index, which then decreased to reach a minimal value after 30 min of exposure to levamisole. In a second experiment, we exposed *lev-10* animals to levamisole for 1 h, and then added nemadipine. Nemadipine induced a decrease of the calcium index in *lev-10* mutants reminiscent to the one observed in wild type (Figs. 1*F* and 4*B*). These two experiments suggest that L-type VGCC activation is

necessary for initial increase of calcium in wild type and maintenance at high level in *lev-10* mutants.

We then tested if L-type VGCC were still present and functional onto the muscle plasma membrane of wild type after 1 h of levamisole exposure. Depolarizing pulses from a holding potential of −60 mV led to the activation of voltage-dependent calcium currents of similar amplitude with or without levamisole treatment (Fig. 4 *C* and *D*). Since the activation properties did not seem to be affected by levamisole treatment, we then tested if inactivation properties were impacted. In *C. elegans*, L-type VGCC exhibit a fast calcium-dependent inactivation and a slow voltage-dependent inactivation (36). Given the slow kinetics of inactivation and an important run-down of the VGCC current (36), we could not perform classical double-pulse protocols to determine the steady-state inactivation curve. Instead, we dissected worms that spent over 1 h on levamisole and measured the membrane potential of the muscle cell as soon as the whole-cell configuration was achieved. We voltage-clamped the cell at this potential and tested the fraction of remaining L-type currents when depolarizing the cell at +20 mV (Fig. 4*E*). This protocol allowed us to monitor the current still available after levamisole exposure. The membrane potentials were significantly more depolarized in wild type than in the clustering-defective mutant *lev-10* (−8 ± 5 mV and −14 ± 6 mV respectively; mean ± SD, *t* test $P = 0.02$). We detected almost no inward current in the wild type, whereas voltage-dependent calcium currents were still present in *lev-10* (Fig. 4*E*). These data indicate that L-type VGCC are probably totally inactivated in the wild type but not in *lev-10* animals, explaining why nonadapting strains enter into flaccid paralysis with low levels of intracellular calcium while their muscle cells are still depolarized by levamisole.

Discussion

The primary incentive of this work was a 40-y-old paradox that emerged from genetic screens showing that *C. elegans* mutants with declustered L-AChRs were less sensitive to the cholinergic agonist levamisole, although they were supposed to have similar amounts of L-AChRs at muscle cell surface. We show here that the L-AChR clustering machinery modifies the properties of levamisole-induced current. In a wild-type context the levamisole-induced current exhibits strong outward rectification; disrupting the interaction with the extracellular clustering scaffold abolishes this peculiar property for a ligand-gated channel from the Cys-loop family, to which L-AChR belongs. Due to rectification, amplitude of levamisole-induced are not significantly different at −60 mV in wild type and in clustering-defective mutants, as previously reported, yet currents are halved in the mutants at membrane potentials close to the resting potential of *C. elegans* muscle cells. As a result, the depolarization induced by levamisole is stronger in the wild type, which leads to the complete inactivation of VGCC, while these VGCC remain partially active in the clustering-defective mutants. VGCC control the excitability of muscle cells and mediate the raising phase of action potentials in *C. elegans*, which does not express canonical voltage-gated sodium channels (34–36). The inactivation of these VGCC has not been studied extensively, mostly because of the fast run-down of the current observed during recordings (36). However, the very slow inactivation that has been reported could be compatible with the kinetics of the calcium concentration decrease and the muscle relaxation observed in the wild type upon prolonged exposure to levamisole. Subsequent events leading to the recovery of locomotion in the clustering-defective mutants after overnight levamisole exposure have not been further investigated. However, it is likely that the dramatic difference in the calcium concentration kinetics between muscle cells of wild type and L-AChR-clustering mutants would participate to long-term modifications of muscle cell homeostasis.

In best characterized examples, outward rectification is explained by intrinsic properties of the channel (e.g., voltage-gated channels), or results from a blockade by extracellular divalent ions (e.g., magnesium for NMDA glutamate receptors). However, outward rectification is a very unusual feature of ionotropic AChR. In vertebrates, currents through AChR exhibit either no rectification, as the muscle AChR (40, 41), or an inward rectification, as most neuronal AChRs (42–46). A few studies have investigated the properties of L-AChR currents at different membrane potentials in *C. elegans* muscle cells. In their pioneering work, Richmond and Jorgensen (18) reported a linear current–voltage relationship from the three recorded cells that were analyzed. We are not able to explain the discrepancy between this report and our present data, since we have observed a strong outward rectification for levamisole-induced currents in wild-type worms, either using our standard saline solution or solutions used in the initial publication (Fig. 3*E*, solution low chloride). L-AChR currents have also been analyzed at the single-channel level; however, the open probability was not quantified at different potentials, thus precluding the possibility to identify a possible voltage-dependent gating of the channels (37, 47). Finally, *C. elegans* L-AChR currents were analyzed after reconstitution of the channels in *Xenopus* oocyte (22). However, as expected in the absence of proteins involved in receptor clustering, the current–voltage relationship was fully linear, in agreement with what we observed in vivo in clustering-defective mutants.

Strikingly, the outward rectification that we observed for L-AChR current in wild type *C. elegans* is highly reminiscent of what was described a long time ago using two-microelectrode voltage-clamp technique in the muscle of the parasitic nematode *Ascaris suum* (48). The current-voltage relationship obtained following application of levamisole or acetylcholine exhibited a nonlinear component at potentials below -30 mV. Harrow and Gration (48) proposed that this rectification could be caused by agonist-induced open channel block. Levamisole action on L-AChR has also been studied at the unitary level on muscle cells from *Ascaris* and from the other parasitic nematode *Oesophagostomum dentatum* (19, 38). In both studies, the unitary conductance remained constant over a wide voltage range, but high concentrations of levamisole (0.1 mM) led to a strong decrease of the open probability, an effect that has been interpreted as voltage-sensitive channel block. However, the outward rectification of L-AChR current does not appear to result from open-channel block in our study. First, rectification of L-AChR in *C. elegans* was also observed with lower doses of levamisole, such as 10 μM (Fig. 3*A*). At this dose, no open-channel block was reported in single-channels recordings of *A. suum* or *O. dentatum* L-AChR currents (19, 38). Second, the rectification was present in our recordings even with acetylcholine application. In *Ascaris*, unitary recordings did not show open-channel block with acetylcholine (49). Third, open-channel block is characterized by a rebound current (a transient current appearing after the removal of the agonist), which we never observed with acetylcholine. Finally, a linear voltage–current relationship was obtained for L-AChR currents from *C. elegans* declustered mutants, which would mean that the open-channel block of acetylcholine and levamisole would be

only effective when L-AChRs are clustered. Such dependence of rectification on the clustering machinery seems incompatible with an open-channel block mechanism.

One hypothesis would be to consider that channel clustering per se explains L-AChR rectification. To our knowledge, very few studies have provided evidence for a link between ligand-gated receptor clustering and electrical properties of a channel, maybe due to a lack of appropriated experimental paradigms. Legendre et al. (50) have described a correlation between the density of glycine receptors and the desensitization kinetics of the receptors when expressed in HEK cells, alone or with gephyrin. In another study, Petrini et al. (51) have observed that desensitization kinetics of $GABA_A$ receptors are modified in cultured hippocampal neurons when microtubules, which are required for clustering, are pharmacologically disrupted. Alternatively, the effects of clustering on receptor electrical properties could be a consequence of interactions between receptors, or between receptors and lipids. Such a model was proposed for the bacterial potassium channel KcsA: clustering/declustering is accompanied by change in competing lipid–protein and protein–protein interactions that would bring changes in the electrical properties of the channel (52).

An alternative hypothesis to explain the rectification of clustered L-AChR would rely on the presence of a component of the scaffolding complex that will confer the rectification property to L-AChRs. In the case of the large conductance calcium-activated voltage-dependent potassium channels, or BK channels, outward rectification has been shown to depend on the extracellular loop of the auxiliary subunit β2, or to a less extent β3 (53–55). Positive residues of the loop might form three electropositive rings at the vicinity of the extracellular entrance that would locally decrease potassium concentration through an electrostatic mechanism. At positive potentials, this phenomenon would be masked by the electric field in favor of potassium efflux. Rectification conferred by the extracellular regions of non-pore-forming proteins might be especially relevant in the case of *C. elegans* L-AChRs. One of the components of the scaffolding machinery might directly interact with the receptor and modify the gating or the permeability of the channel. LEV-10 could be a good candidate because a recent study has shown that the extracellular part of the auxiliary subunit NETO-2, which contains CUB domains as LEV-10, can modulate the inward rectification of the glutamate kainate receptor (56). Deciphering the molecular mechanism of L-AChR outward rectification would require the heterologous reconstitution of the receptor in complex with its clustering scaffold, which we failed to achieve, likely because some components are secreted in culture media and therefore cannot reach sufficient concentrations necessary for complex assembly. We hope that the stunning advances of cryogenic electron microscopy techniques will provide a means to solve the structure of receptors associated with their clustering proteins, either after purification of native receptors or using in situ in vitrified synapses.

In conclusion, our work shows that L-AChR scaffolding complex has a strong effect on the electrical properties of the channel. The outward rectification observed in vivo likely impacts the excitation–inhibition balance of muscle cells and also modifies the organismal response to anti-helminthics. Altogether, our work emphasizes the need to pursue the characterization of ligand-gated channels in their native environment.

Materials and Methods

A list of *C. elegans* strains used in this study is given in *SI Appendix*. All the mutants used were null mutants. Levamisole assays have been performed as previously described (30). In vivo electrophysiology and oocyte experiments were adapted from (22, 36). For calcium data, whole animal expressing GCaMP3.35 have been imaged at low magnification on a Nikon AZ100 multizoom microscope equipped with a digital CMOS camera. We calculated a calcium index corresponding to the variation of pixel number above a threshold defining the upper quartile of pixel intensities measured in the absence of levamisole. Further details about experimental procedures are provided in *SI Appendix*.

Data Availability. All study data are included in the article and/or supporting information.

ACKNOWLEDGMENTS. We thank Luis Briseño-Roa for discussion and reagents, Florence Solari, Thomas Boulin, Christophe Mulle and Owen Randlett for manuscript editing, the *Caenorhabditis* Genetic Center (which is funded by NIH Office of Research Infrastructure Programs, P40 OD010440) for strains, and Olga Andrini for her technical advice on *Xenopus* oocytes handling. This work was supported by the European Research Council to J.L.B. (ERC_Adg C.NAPSE #695295), within the framework of the LABEX CORTEX (ANR-11-LABX-0042) of Université de Lyon, within the program "Investissements d'Avenir" (ANR-11-IDEX-0007) and the AFM Téléthon (Alliance MyoNeurALP). Postdoctoral fellowship of B.B. was supported by a Marie Skłodowska-Curie Individual Fellowship (H2020-MSCA-IF-2017 LEVADAPT #794400). The University of Lyon, the Société Française de Myologie and the AFM-Téléthon contributed to V.L. PhD fellowship.

Author affiliations: [a]Univ Lyon, Université Claude Bernard Lyon 1, CNRS UMR-5284, INSERM U-1314, MeLiS, Institut NeuroMyoGène, F-69008 Lyon, France; and [b]Univ Lyon, Université Claude Bernard Lyon 1, CNRS UMR-5310, INSERM U-1217, Institut NeuroMyoGène, F-69008 Lyon, France

1. S. Tomita *et al.*, Stargazin modulates AMPA receptor gating and trafficking by distinct domains. *Nature* **435**, 1052–1058 (2005).
2. W. Vandenberghe, R. A. Nicoll, D. S. Bredt, Stargazin is an AMPA receptor auxiliary subunit. *Proc. Natl. Acad. Sci. U.S.A.* **102**, 485–490 (2005).
3. S. Choudhary *et al.*, EAT-18 is an essential auxiliary protein interacting with the non-alpha nAChR subunit EAT-2 to form a functional receptor. *PLoS Pathog.* **16**, e1008396 (2020).
4. W. Han *et al.*, Shisa7 is a $GABA_A$ receptor auxiliary subunit controlling benzodiazepine actions. *Science* **366**, 246–250 (2019).
5. E. Jacobi, J. von Engelhardt, Modulation of information processing by AMPA receptor auxiliary subunits. *J. Physiol.* **599**, 471–483 (2021).
6. N. Lei, J. E. Mellem, P. J. Brockie, D. M. Madsen, A. V. Maricq, NRAP-1 is a presynaptically released NMDA receptor auxiliary protein that modifies synaptic strength. *Neuron* **96**, 1303–1316.e6 (2017).
7. M. Tang *et al.*, Neto1 is an auxiliary subunit of native synaptic kainate receptors. *J. Neurosci.* **31**, 10009–10018 (2011).
8. T. Yamasaki, E. Hoyos-Ramirez, J. S. Martenson, M. Morimoto-Tomita, S. Tomita, GARLH family proteins stabilize $GABA_A$ receptors at synapses. *Neuron* **93**, 1138–1152.e6 (2017).
9. W. Zhang *et al.*, A transmembrane accessory subunit that modulates kainate-type glutamate receptors. *Neuron* **61**, 385–396 (2009).
10. T. Boulin *et al.*, Positive modulation of a Cys-loop acetylcholine receptor by an auxiliary transmembrane subunit. *Nat. Neurosci.* **15**, 1374–1381 (2012).
11. J. A. Matta, S. Gu, W. B. Davini, D. S. Bredt, Nicotinic acetylcholine receptor redux: Discovery of accessories opens therapeutic vistas. *Science* **373**, eabg6539 (2021).
12. A. J. Baucum II, Proteomic analysis of postsynaptic protein complexes underlying neuronal plasticity. *ACS Chem. Neurosci.* **8**, 689–701 (2017).
13. S. G. N. Grant, Synapse diversity and synaptome architecture in human genetic disorders. *Hum. Mol. Genet.* **28** (R2), R219–R225 (2019).
14. S. Brenner, The genetics of *Caenorhabditis elegans*. *Genetics* **77**, 71–94 (1974).
15. J. A. Lewis, C. H. Wu, J. H. Levine, H. Berg, Levamisole-resistant mutants of the nematode *Caenorhabditis elegans* appear to lack pharmacological acetylcholine receptors. *Neuroscience* **5**, 967–989 (1980).
16. J. A. Lewis, C. H. Wu, H. Berg, J. H. Levine, The genetics of levamisole resistance in the nematode *Caenorhabditis elegans*. *Genetics* **95**, 905–928 (1980).
17. R. J. Martin, G. Bai, C. L. Clark, A. P. Robertson, Methyridine (2-[2-methoxyethyl]-pyridine]) and levamisole activate different ACh receptor subtypes in nematode parasites: A new lead for levamisole-resistance. *Br. J. Pharmacol.* **140**, 1068–1076 (2003).
18. J. E. Richmond, E. M. Jorgensen, One GABA and two acetylcholine receptors function at the *C. elegans* neuromuscular junction. *Nat. Neurosci.* **2**, 791–797 (1999).
19. A. P. Robertson, H. E. Bjorn, R. J. Martin, Resistance to levamisole resolved at the single-channel level. *FASEB J.* **13**, 749–760 (1999).
20. J. T. Fleming *et al.*, *Caenorhabditis elegans* levamisole resistance genes lev-1, unc-29, and unc-38 encode functional nicotinic acetylcholine receptor subunits. *J. Neurosci.* **17**, 5843–5857 (1997).
21. E. Culetto *et al.*, The Caenorhabditis elegans unc-63 gene encodes a levamisole-sensitive nicotinic acetylcholine receptor α subunit. *J. Biol. Chem.* **279**, 42476–42483 (2004).
22. T. Boulin *et al.*, Eight genes are required for functional reconstitution of the *Caenorhabditis elegans* levamisole-sensitive acetylcholine receptor. *Proc. Natl. Acad. Sci. U.S.A.* **105**, 18590–18595 (2008).

23. P. R. Towers, B. Edwards, J. E. Richmond, D. B. Sattelle, The *Caenorhabditis elegans* lev-8 gene encodes a novel type of nicotinic acetylcholine receptor alpha subunit. *J. Neurochem.* **93**, 1–9 (2005).
24. M. Treinin, Y. Jin, Cholinergic transmission in *C. elegans*: Functions, diversity, and maturation of ACh-activated ion channels. *J. Neurochem.* **158**, 1274–1291 (2021).
25. M. D'Alessandro *et al.*, CRELD1 is an evolutionarily-conserved maturational enhancer of ionotropic acetylcholine receptors. *eLife* **7**, e39649 (2018).
26. S. Eimer *et al.*, Regulation of nicotinic receptor trafficking by the transmembrane Golgi protein UNC-50. *EMBO J.* **26**, 4313–4323 (2007).
27. S. Halevi *et al.*, The *C. elegans* ric-3 gene is required for maturation of nicotinic acetylcholine receptors. *EMBO J.* **21**, 1012–1020 (2002).
28. M. Richard, T. Boulin, V. J. P. Robert, J. E. Richmond, J.-L. Bessereau, Biosynthesis of ionotropic acetylcholine receptors requires the evolutionarily conserved ER membrane complex. *Proc. Natl. Acad. Sci. U.S.A.* **110**, E1055–E1063 (2013).
29. C. Gally, S. Eimer, J. E. Richmond, J.-L. Bessereau, A transmembrane protein required for acetylcholine receptor clustering in *Caenorhabditis elegans*. *Nature* **431**, 578–582 (2004).
30. M. Gendrel, G. Rapti, J. E. Richmond, J.-L. Bessereau, A secreted complement-control-related protein ensures acetylcholine receptor clustering. *Nature* **461**, 992–996 (2009).
31. G. Rapti, J. Richmond, J.-L. Bessereau, A single immunoglobulin-domain protein required for clustering acetylcholine receptors in *C. elegans*. *EMBO J.* **30**, 706–718 (2011).
32. B. Pinan-Lucarré *et al.*, *C. elegans* Punctin specifies cholinergic versus GABAergic identity of postsynaptic domains. *Nature* **511**, 466–470 (2014).
33. X. Zhou *et al.*, The HSPG syndecan is a core organizer of cholinergic synapses. *J. Cell Biol.* **220**, e202011144 (2021).
34. S. Gao, M. Zhen, Action potentials drive body wall muscle contractions in *Caenorhabditis elegans*. *Proc. Natl. Acad. Sci. U.S.A.* **108**, 2557–2562 (2011).
35. P. Liu *et al.*, Genetic dissection of ion currents underlying all-or-none action potentials in *C. elegans* body-wall muscle cells. *J. Physiol.* **589**, 101–117 (2011).
36. M. Jospin, V. Jacquemond, M.-C. Mariol, L. Ségalat, B. Allard, The L-type voltage-dependent Ca2+ channel EGL-19 controls body wall muscle function in *Caenorhabditis elegans*. *J. Cell Biol.* **159**, 337–348 (2002).
37. H. Qian, A. P. Robertson, J. A. Powell-Coffman, R. J. Martin, Levamisole resistance resolved at the single-channel level in *Caenorhabditis elegans*. *FASEB J.* **22**, 3247–3254 (2008).
38. S. J. Robertson, R. J. Martin, Levamisole-activated single-channel currents from muscle of the nematode parasite *Ascaris suum*. *Br. J. Pharmacol.* **108**, 170–178 (1993).
39. T. C. Y. Kwok *et al.*, A small-molecule screen in *C. elegans* yields a new calcium channel antagonist. *Nature* **441**, 91–95 (2006).
40. T. M. Linder, D. M. Quastel, A voltage-clamp study of the permeability change induced by quanta of transmitter at the mouse end-plate. *J. Physiol.* **281**, 535–558 (1978).
41. K. L. Magleby, C. F. Stevens, A quantitative description of end-plate currents. *J. Physiol.* **223**, 173–197 (1972).
42. B. Buisson, M. Gopalakrishnan, S. P. Arneric, J. P. Sullivan, D. Bertrand, Human alpha4beta2 neuronal nicotinic acetylcholine receptor in HEK 293 cells: A patch-clamp study. *J. Neurosci.* **16**, 7880–7891 (1996).
43. I. Forster, D. Bertrand, Inward rectification of neuronal nicotinic acetylcholine receptors investigated by using the homomeric alpha 7 receptor. *Proc. Biol. Sci.* **260**, 139–148 (1995).
44. C. K. Ifune, J. H. Steinbach, Rectification of acetylcholine-elicited currents in PC12 pheochromocytoma cells. *Proc. Natl. Acad. Sci. U.S.A.* **87**, 4794–4798 (1990).
45. A. Mathie, D. Colquhoun, S. G. Cull-Candy, Rectification of currents activated by nicotinic acetylcholine receptors in rat sympathetic ganglion neurones. *J. Physiol.* **427**, 625–655 (1990).
46. C. Mulle, C. Léna, J. P. Changeux, Potentiation of nicotinic receptor response by external calcium in rat central neurons. *Neuron* **8**, 937–945 (1992).
47. D. Rayes, M. Flamini, G. Hernando, C. Bouzat, Activation of single nicotinic receptor channels from *Caenorhabditis elegans* muscle. *Mol. Pharmacol.* **71**, 1407–1415 (2007).
48. I. D. Harrow, K. A. F. Gration, Mode of action of the anthelmintics morantel, pyrantel and levamisole on muscle cell membrane of the nematode *Ascaris suum*. *Pestic. Sci.* **16**, 662–672 (1985).
49. A. J. Pennington, R. J. Martin, A patch-clamp study of acetylcholine-activated ion channels in *Ascaris suum* muscle. *J. Exp. Biol.* **154**, 201–221 (1990).
50. P. Legendre *et al.*, Desensitization of homomeric α1 glycine receptor increases with receptor density. *Mol. Pharmacol.* **62**, 817–827 (2002).
51. E. M. Petrini, P. Zacchi, A. Barberis, J. W. Mozrzymas, E. Cherubini, Declusterization of GABAA receptors affects the kinetic properties of GABAergic currents in cultured hippocampal neurons. *J. Biol. Chem.* **278**, 16271–16279 (2003).
52. M. L. Molina *et al.*, Competing lipid-protein and protein-protein interactions determine clustering and gating patterns in the potassium channel from *Streptomyces lividans* (KcsA). *J. Biol. Chem.* **290**, 25745–25755 (2015).
53. M. Chen *et al.*, Lysine-rich extracellular rings formed by hbeta2 subunits confer the outward rectification of BK channels. *PLoS One* **3**, e2114 (2008).
54. X. H. Zeng, J. P. Ding, X. M. Xia, C. J. Lingle, Gating properties conferred on BK channels by the beta3b auxiliary subunit in the absence of its NH(2)- and COOH termini. *J. Gen. Physiol.* **117**, 607–628 (2001).
55. X.-H. Zeng, X.-M. Xia, C. J. Lingle, Redox-sensitive extracellular gates formed by auxiliary β subunits of calcium-activated potassium channels. *Nat. Struct. Biol.* **10**, 448–454 (2003).
56. L. He *et al.*, Kainate receptor modulation by NETO2. *Nature* **599**, 325–329 (2021).